Quantum Energy Flow and *trans*-Stilbene Photoisomerization: an Example of a Non-RRKM Reaction†

David M. Leitner,*,‡ Benjamin Levine,§ Jason Quenneville,§ Todd J. Martínez,*,§ and Peter G. Wolynes*,⊥

Department of Chemistry and Chemical Physics Program, University of Nevada, Reno, Nevada 89557, Department of Chemistry and the Beckman Institute, University of Illinois at Urbana-Champaign, Urbana, Illinois 61801, and Department of Chemistry and Biochemistry, University of California, San Diego, La Jolla, California 92093

Received: April 28, 2003; In Final Form: July 30, 2003

We apply multireference ab initio quantum chemistry and microcanonical transition state (RRKM) theory with quantum energy flow corrections from local random matrix theory (LRMT) to determine the kinetics of *trans*-stilbene photoisomerization. With a single ab initio potential energy surface and *no* adjustable parameters, simultaneous agreement with experiment of the microcanonical isomerization rates for the d_0, d_2, d_{10}, and d_{12} isotopomers is obtained. We are also able to reproduce the pressure dependence of the thermal rate. Laser cooling effects on the isomerization rate are calculated and found to be quite small. The S_1/S_2 energy gap at the transition state is found to be quite large (0.86 eV), suggesting that nonadiabatic effects are negligible. Using the ab initio results in a simple RRKM theory without corrections for finite quantum energy flow does *not* lead to agreement with experiment. We conclude that non-RRKM effects are essential to understand photoisomerization of *trans*-stilbene and that these can be predicted using LRMT.

1. Introduction

Rice−Ramsperger−Kassel−Marcus (RRKM) theory has very nobly served as the foundation for calculating rates of unimolecular reactions.[1] However, a growing body of experimental work[2−8] on the rates of conformational change of molecules indicates that RRKM theory alone cannot always completely account for the kinetics. For example, recent studies of dipeptide isomerization in molecular beams reveal the possibility of specific pathways to transition states controlling the rate,[2] a process not addressed by RRKM theory. Measurements of conformational isomerization rates for cyclohexanones in gas phase[3] and cyclohexane in solution[4] are much slower than predicted by RRKM theory. Molecular beam studies of several modest-sized organic molecules, such as 2-fluoroethanol and allyl fluoride, by Pate and co-workers[5−8] reveal that intramolecular energy flow and isomerization rates are extremely slow for these molecules even at energies significantly higher than the barrier energy. Some of the earliest hints at these limitations of RRKM theory were found in the measured rates of *trans*-stilbene photoisomerization in molecular beams[9,10] and in vapor[11,12] that are generally lower than the RRKM predictions. Calculations and simulations[13−16] lead one to conclude that, at least in the aforementioned molecules, dynamical corrections to RRKM theory are essential in order to capture even qualitative variations of the reaction rates with energy or pressure. Indeed, Leitner and Wolynes[16] have argued that dynamical corrections to RRKM calculations should be generally important in predicting rates of unimolecular reactions of large molecules over low barriers, since vibrational modes of the reactant are barely excited at such low energies. Quantum mechanical energy flow in to and out of an activated complex is, at low energy, often too slow to compete with the faster vibrational time scale for transition from the activated complex to product.

Many of the studies described above involve reactions that take place in the ground electronic state. Reliable potential energy surfaces required to study the reaction dynamics of these systems are thus available, and the conclusion that dynamical corrections are important for these reactions has not met with controversy.[13,14,17] However, photoisomerization of *trans*-stilbene occurs on an excited electronic state potential energy surface. This raises concerns about theoretical calculations of the rate owing to uncertainties about excited state surfaces. RRKM calculations using nearly all available potential energy surfaces for excited state *trans*-stilbene overestimate the rate. It has been pointed out for some time that if RRKM predictions are corrected for limited or slow vibrational energy flow, they can be brought into line with experiment,[15,18] a suggestion that has since been supported by calculations of energy flow rates in stilbene.[16] Still, the origin of the discrepancy as being due to non-RRKM effects has been debated for this singular case of stilbene isomerization,[19,20] many authors preferring to make modifications of the surfaces that allow better agreement with pure RRKM theory.

Early semiempirical QCFF/PI with single-excitation configuration interaction (CI) quantum chemical calculations by Warshel[21] provided the vibrational frequencies needed for the first RRKM calculations[18] on stilbene photoisomerization. In this and many other subsequent calculations, the frequencies of the activated complex were assumed to remain the same as those of the reactant, with the sole exception of the reaction coordinate. When compared with measured rates in supersonic jets, the RRKM estimates for the rate were found to be about an order of magnitude too large. A number of possible reasons for this discrepancy have been investigated to various degrees

† Part of the special issue "Charles S. Parmenter Festschrift".
‡ University of Nevada, Reno.
§ University of Illinois at Urbana−Champaign.
⊥ University of California, San Diego.

10.1021/jp0305180 CCC: $25.00
Published on Web 09/12/2003

by many workers. Concentrating first on the possibility that the adiabatic RRKM treatment is appropriate, there are four areas of uncertainty: (1) the reactant vibrational frequencies may be inaccurate, (2) the activated complex vibrational frequencies may differ significantly from those of the reactant, (3) the barrier height may be in error, and (4) the reaction coordinate may have been misidentified. We comment on the first two of these possibilities together and then on the last two.

There have been relatively few attempts to generate improved vibrational frequencies for the reactant, primarily because of the difficulty involved in such calculations for excited electronic states. Negri and Orlandi used a semiempirical QCFF/PI method[22] including double excitations in the CI to generate S_1 frequencies for both the reactant and transition state which were used in rate calculations.[23] They noted that the frequencies did change noticeably from reactant to transition state but did not directly quantify the effect of neglecting these frequency changes. Frederick and co-workers used the experimental absorption spectrum to modify an empirical force field which they used in studies of ultrafast stilbene photophysics.[24,25] They did not address the issue of isomerization rates from the trans isomer. However, Gershinsky and Pollak subsequently noted that the S_1 frequencies derived from this empirical force field were sufficiently different from past results to change the RRKM predictions. Indeed, they showed that an RRKM model based on these frequencies and accepted estimates of the barrier height and reaction coordinate frequency led to rates which agreed with experiment.[19] Three ab initio sets of S_1 frequencies have recently been presented,[20,26,27] but only one of these[20] has been used in rate calculations. Two of the ab initio calculations[20,27] use single-reference single-excitation CI (CIS) methods,[28] which are of uncertain reliability for excited states. The other uses a more reliable multireference complete active space (CASSCF) method, but only a subset of the frequencies was presented due to numerical difficulties.[26] As shown below, most of these S_1 frequencies are not very different from each other. The exception is the set used by Gershinsky and Pollak, which contains many low-frequency modes.

Troe has championed the last two possibilities to explain the rates in a strict RRKM framework—errors in the barrier height and misidentification of the reaction coordinate frequency. By treating the barrier height as an adjustable parameter, and choosing a reaction coordinate frequency of 88 cm^{-1}, he was able to fit the observed rates to an RRKM model.[29] The resulting barrier height was in reasonable agreement with experimental threshold measurements[9] ($\approx$1200 cm^{-1}), but the reaction coordinate frequency was significantly lower than other assignments[30] which generally fall in the range of 200−400 cm^{-1}. Furthermore, to explain the turnover in rates at low pressures observed in fluorescence decay measurements for *trans*-stilbene in ethane, the reaction coordinate frequency must be greater than 160 cm^{-1}.[31] More recently, Schroeder, Steinel, and Troe have combined a set of S_1 frequencies obtained from an ab initio CIS method with reassignment of the reaction coordinate to a 25 cm^{-1} mode.[20] Again taking the barrier height to be an adjustable parameter, good agreement between RRKM and observed rates is obtained, and the resulting barrier height is in reasonable agreement with the threshold value.

Given only the supersonic jet data for the usual isotopomer of *trans*-stilbene, one could conceivably be satisfied that RRKM can explain the isomerization rate with appropriate, but perhaps questionable, choices of the input parameters. However, there are two other crucial experiments. First, rate measurements in supersonic jets on isotopomers[10,32] showed an ordering of the isomerization rates which was in conflict with that expected on the basis of the density of states. The reactant density of states is expected to rise in the order d_0, d_2, d_{10}, d_{12} and hence the reverse ordering is predicted for the isomerization rate. However, the observed ordering of the rates interchanges d_{10} and d_2. Standard RRKM theory cannot explain this ordering unless one allows for an isotope-dependent barrier, perhaps arising from tunneling or zero-point energy effects. Second, Balk and Fleming found that the rate of stilbene isomerization increases by a factor of about 13 with pressure in methane buffer gas for pressures from 1 to 100 atm.[11,12] RRKM theory predicts that the reaction rate should not vary with pressure in this range, although there have been attempts to rescue RRKM by invoking explicitly pressure-dependent barriers.[33]

Thus, we turn to the alternative explanation for the failure of standard RRKM theory when applied to stilbene isomerization—the dynamical assumptions of the theory are violated. In general, there are two distinct ways for a process to violate the standard RRKM assumptions. First, nonadiabatic effects could be operative in the transition state region. This explanation was put forward already in the first RRKM calculations[18] and was further investigated by Negri and Orlandi.[23] While this could reconcile theory and experiment for the jet experiments, it leaves the pressure dependence of the rate unexplained. Second, there might be restricted or slow intramolecular vibrational energy redistribution (IVR). Nordholm[15] pointed out that the overestimate of the rate by RRKM theory would be consistent with measured rates of intramolecular vibrational redistribution (IVR) in stilbene in the neighborhood of the barrier energy, which are on the order of 1 ps^{-1}. Such an IVR rate is considerably slower than the frequency of crossing the barrier along the reaction coordinate, which should be at least 5 ps^{-1}.[31] When relaxation is slow, we must include a correction to the RRKM theory prediction for the rate due to the finite ($\approx$1 ps^{-1}) rate of IVR. In this case of sluggish IVR, the pressure dependence may be explained because IVR is enhanced by collisions, thereby speeding up the rate.

The case for non-RRKM effects in stilbene photoisomerization was seemingly settled by a study of two of the present authors in 1997. Leitner and Wolynes[16] used an approximate theory of IVR rates along with one of the available potential surfaces[23] to estimate the non-RRKM corrections both for the isomerization of d_0 stilbene in molecular beam and pressure-dependent bulb experiments. Reasonable agreement with experiment was found without any adjustments of the potential surface from that used in earlier RRKM predictions.

But this was not the end of the story. In the same year as the Leitner−Wolynes work, Gershinsky and Pollak proposed a different resolution of the experimental puzzles. As mentioned above, they noticed that one of the recent potential energy surfaces generated for stilbene[25] had much more lowering of the S_1 vibrational frequencies (compared to S_0) than previously thought. Modifying the surface in this way allows a good fit of RRKM theory to the isolated molecule experiments for the d_0 isotopomer, which was the only one for which rates were calculated. They recognized that the pressure dependence would still pose a problem for standard RRKM theory. A novel resolution appeared to this puzzle: Gershinsky and Pollak suggested that the preponderance of low S_1 frequencies could lead to the importance of a previously unconsidered effect, laser cooling, which could accommodate the observed pressure dependence.

Cooling by photoexcitation has been observed by Beddard et al.[34] in naphthalene. It can be crudely understood as arising

from an adiabatic expansion of the available phase space of the molecule if mode frequencies are lowered upon photoexcitation. Once the internal vibrations are cooled by excitation, the buffer gas can warm these degrees of freedom, thus enhancing the isomerization rate. Interestingly, Leitner and Wolynes showed that the same softening of vibrations invoked by Gershinsky and Pollak would, if correct, increase IVR rates and would indeed lead to RRKM behavior, but the predicted IVR rates would then be in conflict with earlier measurements[35] by Zewail and co-workers.

In recent years evidence for cooling in *trans*-stilbene has been found by Warmuth et al.,[36] who observed a dependence of the isomerization rate on the laser excitation frequency in bulb experiments. Just such an effect would be expected on the basis of the cooling mechanism. However, the amount of cooling needed to account for their observations is not as large as needed to explain the overall rates of isomerization.

More recently Schroeder, Steinel, and Troe[20] have disputed the existence of both non-RRKM effects and of significant laser cooling effects in *trans*-stilbene. They used a single-reference ab initio method (CIS) to compute S_1 frequencies which were employed in an RRKM model, treating the barrier heights as isotope-dependent adjustable parameters. They further identified the lowest frequency reactant mode as the reaction coordinate—with a frequency of 25 cm^{-1}. The resulting rates agree well with bulb and beam experiments for all four isotopomers, but the barrier heights show unexpected isotope effects. The barriers obtained for d_0, d_2, and d_{12} are 1150 ± 5 cm^{-1} but the d_{10} barrier is almost 100 cm^{-1} lower. Troe and Schroeder provide no explanation why three of the isotopomers should have essentially the same effective barrier and the fourth should be significantly different. Thus, they also suggest the experiments may not be sufficiently accurate for the d_{10} isotopomer. On the other hand, the pressure effects cannot be explained in this standard RRKM model, even using the revised barrier parameters, without invoking a further dependence of the barrier height on pressure. Such a variation is conceivable if van der Waals complexes with the buffer gas are formed, and would further explain the dependence of the isomerization rates on buffer gas composition.[31] However, in the absence of explicit calculations of the barrier heights in such van der Waals complexes, this must be regarded as an a posteriori fit. Despite requiring ad hoc adjustments such as unnatural isotope dependence of the isomerization barriers and unquantified clustering effects and the need to ignore previous arguments against a reaction coordinate frequency below 200 cm^{-1}, Schroeder et al. claim that RRKM theory with these additions agrees perfectly with experiment and therefore demonstrates the validity of standard RRKM theory for *trans*-stilbene isomerization and is "certainly of textbook quality."[20] They argue that the level of agreement of their calculations with experiment "casts considerable doubt on earlier suggestions such as reversible reaction, incomplete IVR, electronically nonadiabatic reaction, or other mechanisms."[20]

In an effort to help resolve the controversy about this historically important system we have reexamined the potential energy surface for photoexcited stilbene using modern quantum chemical methods. In this article, we present new vibrational frequencies for the S_1 trans minimum and the trans → cis isomerization transition state of stilbene. Using these new frequencies and the computed barrier height, we calculate the RRKM isomerization rate and dynamical corrections to the RRKM rates. The mode density that we calculate is similar to that found for most other potential energy surfaces proposed for S_1 *trans*-stilbene and indeed is very close to the original results of Warshel.[21] The barrier frequency is in the 500−600 cm^{-1} range, consistent with many previous estimates and spectroscopic data. These data are also sufficient to examine the cooling effect proposed by Gershinsky and Pollak as a way to resolve the discrepancy between RRKM theory and experiment. We estimate the temperature of stilbene at low pressures by comparing the frequencies of the S_0 and S_1 states of stilbene, as suggested by Gershinsky and Pollak.[19] We find cooling on the order of 3 K, which would have a small though possibly observable effect on the rate at low pressure.

In the following section, we discuss the ab initio results relevant to *trans*-stilbene isomerization. In section 3, the ab initio data are used to calculate the RRKM estimate for the reaction rate. We then compute the rate of energy flow from transition states to nonreactive states of stilbene and introduce these rates into a dynamical correction to the RRKM estimate for the isomerization rate. We compare these results with measured rates of photoisomerization for the d_0, d_2, d_{10}, and d_{12} isotopomers in supersonic jets.[10,32] In section 4, we use the microcanonical reaction rates to calculate the thermal rate of photoisomerization, and compare with the Balk−Fleming data.[11,12] We also estimate the nonequilibrium temperature of stilbene in the S_1 state, as suggested by Gershinsky and Pollak,[19] to determine any effect the excited-state cooling might have on the thermal rate at low pressure. We conclude in section 5 with our view of the current status of RRKM theory and its corrections for this system.

2. Ab Initio Calculations on *trans*-Stilbene

We have used a state-averaged[37] CASSCF method,[38] equally weighting S_0 and S_1, with two electrons in two orbitals for the electronic wave function, referred to as SA-2-CAS(2/2) in the following. Corrections for dynamical electron correlation are included with time-dependent density functional theory[39,40] (TDDFT) or internally contracted second-order perturbation theory,[41] hereafter denoted PT2. The valence double-ζ 6-31G basis set was used[42] and symmetry constraints were not imposed on either geometries or electronic wave functions. All multireference calculations were performed with the MOLPRO package.[43] The Gaussian98 program[44] is used for CIS and TDDFT calculations. The force constant matrix for normal-mode analysis is computed by numerical central differences of analytic gradients, with a step size of 0.001 bohr. All frequencies have been scaled by 0.9 in the usual way.[45] Previously calculations were reported on the form of the resulting potential energy surfaces with emphasis on the region near the low-lying conical intersections which promote $S_1 \rightarrow S_0$ quenching.[46] Full details of the geometry of the SA-2-CAS(2/2) transoid S_1 minimum were given in that work.

The frequencies resulting from normal-mode analysis at the S_0 and S_1 trans minima are given in Table 1. In Figure 1, we compare the S_1 frequencies determined here and in previous work, by plotting the total number of modes up to a given frequency as a function of frequency, i.e., the integrated mode density. It is quite clear that the distribution of frequencies from the original work of Warshel[21] is supported by both single-reference and multireference quantum chemistry methods. On the other hand, the frequency distribution of Gershinsky and Pollak is noticeably different from all others, and surely lies outside the uncertainty in the frequencies from either of the ab initio methods.

To find the trans → cis isomerization transition state, we have scanned the torsion angle, minimizing the S_1 energy in all other coordinates and using the SA-2-CAS(2/2) electronic wave function. The torsion angle is defined such that the molecule

TABLE 1: SA-2-CAS(2/2) Vibrational Frequencies for d_0 *trans*-Stilbene at the Ground and Excited State Minimum and the Trans → Cis Isomerization Transition State Geometry[a]

S_0 min	S_1 min	S_1 TS	S_0 min	S_1 min	S_1 TS
22	25	54	1063	1043	1058
58	51	66	1082	1078	1068
58	73	72	1085	1084	1080
106	127	137	1149	1167	1114
186	182	182	1152	1167	1166
218	233	272	1186	1191	1168
263	285	294	1194	1193	1181
325	291	321	1199	1202	1190
419	412	413	1210	1233	1208
420	417	416	1239	1273	1230
448	462	473	1242	1322	1293
502	473	510	1307	1329	1306
543	486	522	1337	1337	1327
544	529	567	1361	1365	1333
632	614	***607i***	1370	1385	1368
635	620	618	1460	1444	1401
652	634	623	1469	1457	1451
715	665	636	1509	1483	1464
719	669	678	1512	1499	1482
772	755	685	1597	1530	1497
798	768	762	1603	1535	1537
809	794	790	1617	1593	1550
866	814	799	1623	1595	1593
885	828	823	1655	1677	1604
886	845	834	3002	3015	2873
912	850	860	3007	3017	2977
968	878	883	3013	3021	3008
984	922	912	3013	3021	3012
997	927	963	3020	3023	3021
1001	980	981	3021	3027	3029
1004	987	990	3031	3036	3030
1029	1002	1006	3032	3037	3033
1030	1003	1006	3042	3053	3041
1032	1019	1016	3042	3053	3049
1032	1020	1032	3051	3069	3053
1063	1043	1039	3052	3070	3064

[a] All frequencies have been scaled by 0.9.

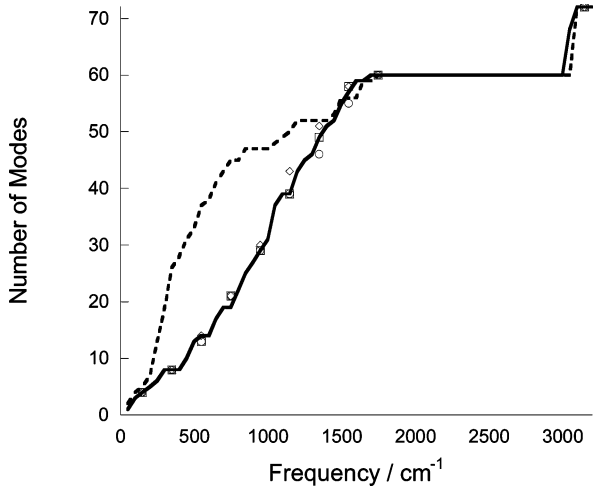

Figure 1. Integrated vibrational density of states from various models for the *trans*-stilbene minimum on S_1. Results from the SA-2-CAS(2/2) ab initio method in this work are presented as a solid line. Results from previous work are presented as symbols − diamonds (Schroeder, Steinel, and Troe[20]), circles (Warshel[21]), and squares (Negri and Orlandi[23]). The results of Gershinsky and Pollak[19] are shown as the dashed line. All semiempirical and ab initio methods are in reasonable agreement and find fewer low-frequency modes than the Gershinsky/Pollak results.

is purely twisted about the ethylenic bond with no pyramidalization of the ethylenic carbon atoms. Specifically, this is

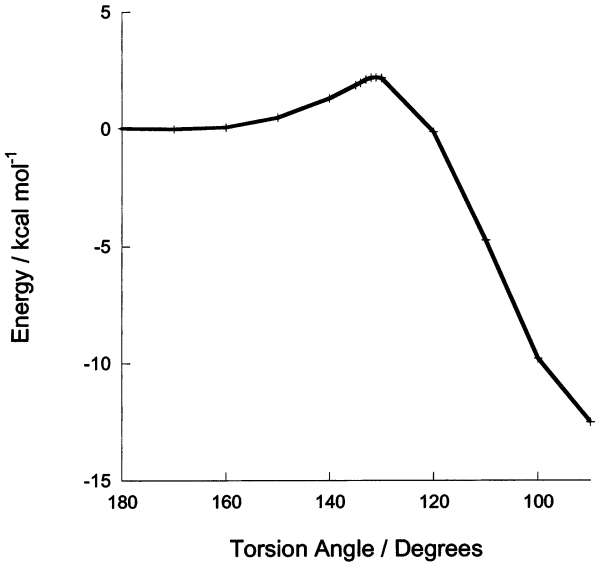

Figure 2. S_1 potential energy curve of *trans*-stilbene for fixed torsion angle. All other coordinates are optimized at each point under the constraint of pure torsion (with no pyramidalization of the ethylenic carbon atoms). The zero of energy corresponds to the S_1 trans minimum.

done by constraining the C_{Ph}-C═C−C_{Ph}, H−C═C−C_{Ph}, and C_{Ph}−C═C−H dihedral angles. The resulting potential energy curve is shown in Figure 2, and the transition state for isomerization is found with a torsion angle of 131°. Strictly speaking this is an approximate transition state, since it does not admit any pyramidalized character on the ethylenic carbon atoms. Normal-mode analysis shows that it has exactly one imaginary frequency. The geometry of the transition state structure is shown in Figure 3, which also gives geometric information about the S_1 minimum for comparison. The changes between the S_1 minimum and S_1 transition state geometries are very minor, apart from the ethylenic torsion angle. Note that although the S_1 trans minimum is not found to be perfectly planar, the SA-2-CAS(2/2) potential energy is very insensitive to ethylenic torsion between 180 and 160°.

The reaction coordinate mode is shown in Figure 4, where a preponderance of hydrogen motion is clearly visible. Furthermore, one can see that there is very little motion of the phenyl rings at the transition state. Thus, the reaction coordinate at the transition state does not fit the usual picture of a rigid torsion about the ethylenic bond. This is a particularly important point in light of previous efforts to define the reaction coordinate by finding the reactant normal mode which most closely resembled rigid ethylenic torsion. Furthermore, the large degree of hydrogen motion implies large isotopic shifts in the barrier height from zero-point energy considerations. In Table 2, we present the frequency of the reaction coordinate at the transition state and the zero-point energy correction to the barrier for the d_0, d_2, d_{10}, and d_{12} isotopomers. The zero-point energy correction differs by roughly 100 cm^{-1} for the d_2 and d_{12} isotopomers which have the ethylenic positions deuterated.

The barrier height obtained at the SA-2-CAS(2/2) level is 790 cm^{-1} before ZPE corrections. However, barriers are notoriously difficult to calculate accurately, especially on excited states. In particular, it is very important to include both static and dynamic electron correlation effects. Thus, we investigate the role of electron correlation here. The values for this barrier obtained by evaluating the energy using different electronic structure methods at the minimum and transition state geometries obtained with SA-2-CAS(2/2) are given in Table 3. The CIS value is of interest primarily because this method had been

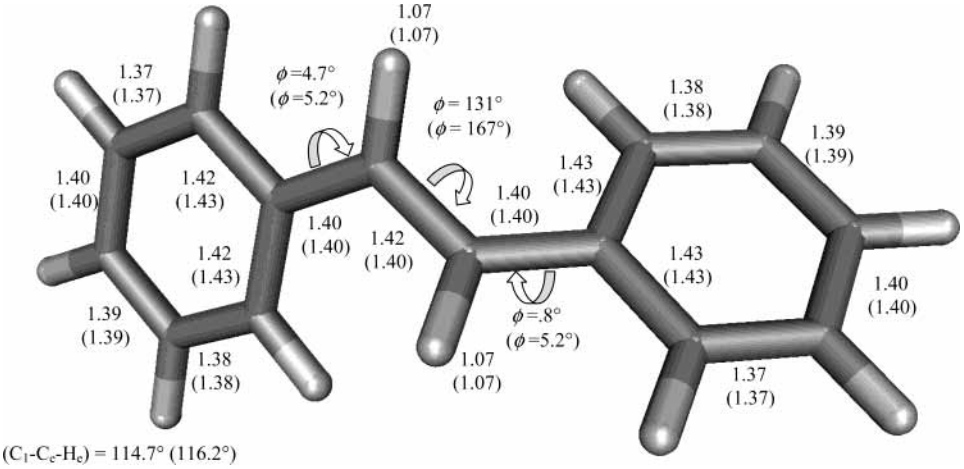

Figure 3. Geometry of the best approximate transition state for cis−trans isomerization of stilbene on S_1. Selected geometrical parameters are given, along with corresponding geometrical parameters for the translike minimum on S_1 in parentheses.

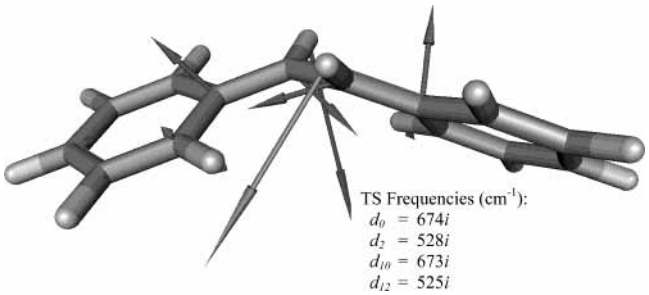

Figure 4. Mode corresponding to reaction coordinate at the isomerization transition state. There is exactly one imaginary frequency, indicated in the inset for each isotopomer. The mode shown corresponds to the d_0 isotopomer.

TABLE 2: ZPE Correction to Barrier Height, Reaction Coordinate Frequency, and IVR Thresholds for Isomerization of *trans*-Stilbene on S_1[a]

	ZPE correction to barrier height (cm^{-1})	TS frequency (cm^{-1})	IVR threshold (cm^{-1})
d_0	597	607i	1275−1325
d_2	493	475i	1225−1275
d_{10}	602	606i	1075−1125
d_{12}	496	473i	1025−1075

[a] The ZPE corrections should be subtracted from the barrier heights in Table 3.

TABLE 3: Computed Barrier Height (without ZPE Corrections) for Excited State Stilbene Isomerization Using Geometries Obtained from SA-2-CAS(2/2) and the 6-31G Basis Set

method	barrier (ΔE)/cm^{-1}
CIS	635
TDDFT (B3LYP)	442
SA-2-CAS(2/2)	790
SA-2-CAS(2/2)-PT2	341
SA-5-CAS(14/12)[a]	1493
SA-5-CAS(14/12)[b]	1796
extrapolated[c]	1347

[a] S_1 minimum geometry from SA-2-CAS(2/2) is used. [b] S_1 minimum geometry from SA-5-CAS(14/12) is used. [c] $\Delta E_{\text{extrapolated}} = \Delta E_{\text{SA-5-CAS(14/12)}} - \Delta\Delta E^{\text{dynamic-correlation}}_{\text{SA-2-CAS(2/2)}}$, where $\Delta\Delta E^{\text{dynamic-correlation}}_{\text{SA-2-CAS(2/2)}} = \Delta E_{\text{SA-2-CAS(2/2)-PT2}} - \Delta E_{\text{SA-2-CAS(2/2)}}$ and the SA-5-CAS(14/12) geometry is used for the S_1 minimum.

previously employed[20] in RRKM rate calculations of stilbene isomerization, although the earlier work stopped short of computing the barrier, which was instead treated as a fitting parameter. As expected, and as is evident from the TDDFT and SA-2-CAS(2/2)-PT2 results, accounting for dynamic electron correlation lowers the barrier. However, static correlation (recovered using large active spaces) stabilizes conjugated forms of polyenes and can therefore strongly affect barriers for processes which involve breaking conjugation. Thus, we have carried out calculations with an active space including all π electrons and 12 of the valence π orbitals. In this case, the $\pi \rightarrow \pi^*$ state is S_4, so we average over the five lowest electronic states, i.e SA-5-CAS(14/12). As expected, the barrier increases (1493 cm^{-1}) compared to the SA-2-CAS(2/2) estimate. Reoptimizing the excited state trans minimum further increases the computed barrier to 1796 cm^{-1}. To simultaneously include static and dynamic correlation effects, one would require at least a SA-5-CAS(14/12)-PT2 calculation. As this is presently computationally infeasible, we have estimated the combined static/dynamic correlation effect using a composite,[47] also known as focal point,[48] method. The dynamic correlation correction to the barrier height is computed from the SA-2-CAS(2/2) and SA-2-CAS(2/2)-PT2 results-dynamic correlation lowers the barrier by 449 cm^{-1}. This correction is applied to the best SA-5-CAS(14/12) estimate of 1796 cm^{-1}, yielding the barrier height denoted "extrapolated" in Table 3. This result is expected to be somewhat too low because of some double counting of dynamic correlation—it is difficult to separate static and dynamic correlation contributions cleanly. Further uncertainty in the barrier height is expected from the finite basis set and truncated perturbation expansion. As there are few documented cases where quantum chemistry has been used to compute experimentally known barrier heights on excited-state surfaces, it is not possible to give a precise estimate of the uncertainty. However, an error of 100 cm^{-1} would not be surprising. Efforts to compute this barrier more accurately will be welcome in the future. However, one can see quite clearly that there is a tendency for all methods to predict a barrier height which is significantly lower than the previous estimates which equated the barrier height to the measured energy threshold. Indeed, our best barrier height is significantly lower than previous estimates: 750 cm^{-1} after ZPE correction compared to the energy threshold of 1100−1200 cm^{-1}. This would seem to portend disaster in the isomerization rates if taken literally, but amazingly we will see that this is not so.

In Figure 5, we show the normal modes of the S_1 minimum with at least 3% projection onto the reaction coordinate mode at the transition state. The first point here is that the reaction coordinate is far from a pure reactant mode, and 26% of the

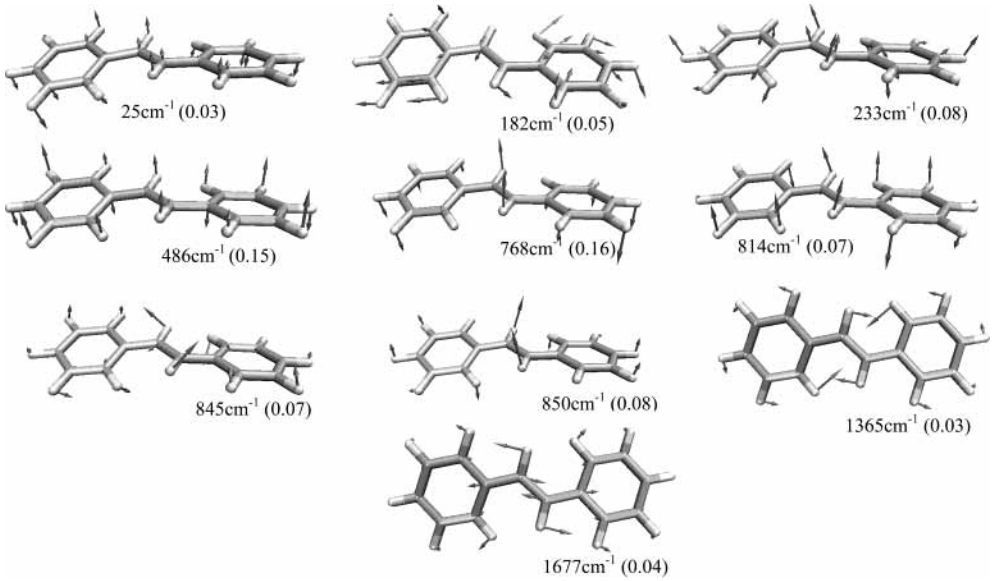

Figure 5. Normal modes and frequencies of the d_0-stilbene S_1 trans minimum. Only modes with squared projection (given in parentheses) onto the reaction coordinate of 0.03 or greater are shown. The 25 cm^{-1} mode identified by Schroeder, et al. has significant ethylenic torsion character but an almost insignificant contribution to the reaction coordinate at the transition state.

reaction coordinate is spread over the remaining 62 modes which are not shown. The mode which Schroeder, Steinel, and Troe have identified as the reaction coordinate is indeed the one with the most resemblance to a rigid ethylenic torsion, yet it has only a 3% contribution to the reaction coordinate. Indeed, the dominant contributions come from the modes at 486 and 768 cm^{-1}: the out-of-phase combination of these modes cancels much of the phenyl contribution. In short, according to our calculations, the mode Schroeder, et al. identify as the reaction coordinate is relevant, but it is no more relevant than the modes at 1365 and 1677 cm^{-1}, which are almost purely in plane.

To inquire into the possibility of nonadiabatic effects, we have computed the S_1-S_2 energy gap at the transition state using SA-3-CAS(2/2). The gap is found to be 1.6 eV. Including dynamic correlation effects with second-order perturbation theory, SA-3-CAS(2/2)-PT2, reduces this gap to 0.86 eV. While one expects this to be somewhat overestimated because of the small active space, it is nevertheless large enough that we can rule out nonadiabatic effects at the identified transition state with confidence. With the transition state, barrier height, reaction coordinate, and frequencies in hand, we now proceed to address the isomerization rates.

3. Energy-Dependent Photoisomerization Rate of *trans*-Stilbene

RRKM theory expresses the microcanonical rate of isomerization as[1]

$$k(E) = \frac{N^+(E - E_0)}{h\rho(E)} \tag{1}$$

where $N^+(E - E_0)$ is the number of vibrational states of the transition state with excess energy less than or equal to $E - E_0$, $\rho(E)$ is the density of vibrational states of the reactant at energy E, and h is Planck's constant. With the vibrational frequencies of the reactant, we can calculate the density of states and N^+ by direct count and calculate the isomerization rate. This is the RRKM estimate. An inherent assumption embodied in eq 1 is that the reactant remains in microcanonical equilibrium at all times. RRKM theory assumes reactants that are poised to react will do so on a time scale of the barrier crossing frequency. For this to be true and for the reactant population to remain in equilibrium, the transition states following reaction must be repopulated either by IVR or by collisions on a time scale much faster than the vibrational frequency for crossing the barrier. For now, we assume that only IVR can repopulate transition states of stilbene.

In this case, we must introduce a correction to RRKM theory that accounts for the finite time to redistribute energy within the reactant. If k_{IVR} is the IVR rate, then the isomerization rate becomes[15,16]

$$k(E) = \kappa(E)k_{RRKM}(E) \tag{2a}$$

$$\kappa(E) = \frac{k_{IVR}(E)}{k_{IVR}(E) + \nu_R(E)} \tag{2b}$$

We note that this expression assumes IVR is a simple exponential process. This is a crude assumption. Both experiment and LRMT theory suggest IVR is a multiexponential or power law process.[49] Clearly the magnitude of the reaction mode frequency, ν_R, plays a critical role in the extent to which dynamical corrections to RRKM theory are involved. This mode frequency has often been associated with the vibrational frequency of the mode that most closely coincides with the reaction path, i.e., a torsional motion about the ethylenic bond. As shown in Figure 5, our calculations find that quite a few modes participate in this motion, implying that it is a poor approximation to associate ν_R with a single reactant mode. Modes of frequencies in the range of about 200−400 cm^{-1} have generally been assigned to those corresponding to this motion,[30] and numerous RRKM calculations over the past 20 years have used mode frequencies in this range or higher.[50] The only exception is the work of Troe and co-workers,[20,29] discussed previously. Because we have located the transition state and carried out a normal-mode analysis (see Table 1 and Figure 4), we avoid any uncertainties about the reactant mode corresponding to the reaction coordinate and ν_R is given as the imaginary frequency at the transition state. This is 607 cm^{-1} for the d_0 isotopomer, and in the calculations that follow, we use the imaginary frequency for the appropriate isotopomer (see Table 2) for ν_R.

One necessary, though not sufficient, criterion for the RRKM limit to be reached is that there be unrestricted IVR at energies above the barrier. We therefore first calculate the IVR threshold using local random matrix theory (LRMT),[51] a theory that establishes criteria for vibrational energy to flow quantum mechanically. The foundation of LRMT is a mapping of the problem of energy flow in a quantum mechanical system of many coupled nonlinear oscillators to that of single-particle quantum transport on a disordered lattice.[52] A vibrational state space is defined in terms of the occupation numbers of the nonlinear oscillators in the system, so that each state can be thought of as a site on a many-dimensional lattice. Low-order anharmonicity couples a given site to nearby sites on the lattice, and the energies of these coupled sites can be taken to be essentially random from a distribution characterized by the range of oscillator frequencies. Logan and Wolynes[52] found a transition for energy to flow globally on the energy shell that occurs at a critical value of the product of the anharmonic coupling, v, and local density of states, ρ_{loc}. For smaller values of the product $\Theta = 2\pi/3(v\rho_{loc})^2$, energy is localized, the extent of which may be computed by LRMT;[51] for values of Θ sufficiently above the critical value, energy flow rates in the vibrational state space can be estimated by the golden rule (see eq 5). Good agreement between LRMT and with measured values has been found for the IVR transition and IVR rates in a number of organic molecules.[51]

In an earlier LRMT calculation using the vibrational frequencies of Negri and Orlandi,[23] we found the IVR threshold to lie around 1300 cm^{-1}, close to previous estimates of the isomerization barrier. We again use LRMT to estimate the IVR threshold, this time using the new vibrational frequencies presented in Section 2. The IVR transition lies at an energy where the local density of states coupled anharmonically to states on the energy shell, times the strength of anharmonic coupling, is of order 1. More specifically, IVR is unrestricted when[51,52]

$$\sqrt{\frac{2\pi}{3}}\sum_Q \langle |V_Q|\rangle \rho_Q \geq 1 \tag{3}$$

We obtain the local density of states coupled by all orders of anharmonicity to any given state on the energy shell by direct count using the frequencies provided in the previous section. Gruebele and co-workers have shown that anharmonic matrix elements, $V_{ii'}$, coupling states $|i\rangle$ and $|i'\rangle$ can be very well estimated using some rather simple formulas once the vibrational frequencies are known,[49,53−55]

$$V_{ii'} = \prod_\alpha R_\alpha^{n_\alpha} \tag{4a}$$

$$R_\alpha \approx \frac{a^{1/Q}}{b}(\omega_\alpha \bar{\nu}_\alpha)^{1/2} \tag{4b}$$

$$Q = \sum_\alpha n_\alpha \tag{4c}$$

where n_α is the occupation number difference between two normal modes, α' and α, for the basis states $|i\rangle$ and $|i'\rangle$, $n_\alpha = \upsilon_{\alpha'} - \upsilon_\alpha$; $\bar{\nu}_\alpha$ is the geometric mean of the occupation number of mode α in the two states, $|i\rangle$ and $|i'\rangle$; a and b are constants. If $V_{ii'}$ is expressed in cm^{-1}, then $a \approx 3000$ and $b \approx 200-300$. We use $a = 3050$ and $b = 230$ in our calculations. Gruebele's work has shown that eq 4 provides good estimates for anharmonic coupling matrix elements for various moderate-sized branched and cyclic organic compounds.[49,53−55]

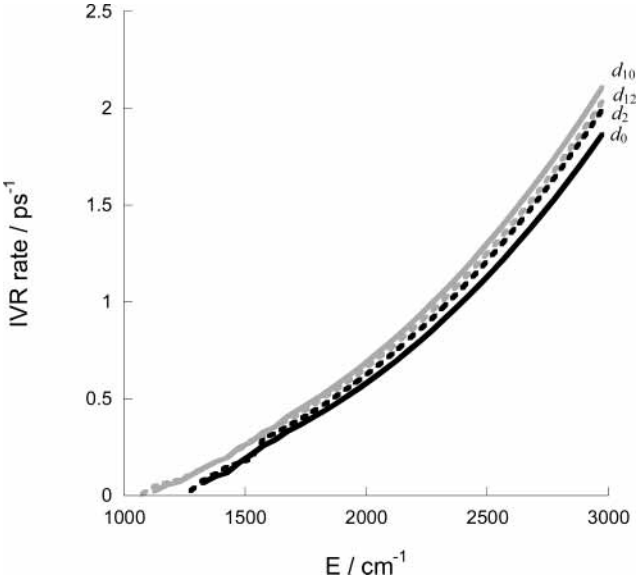

Figure 6. LRMT IVR rates for energy transfer to the S_1 isomerization reaction coordinate for four isotopomers of *trans*-stilbene. The energy flow rates are quite similar for all isotopomers and do not follow the order observed for the isomerization reaction rate.

Using eqs 3 and 4, we find the IVR transition for stilbene lies near 1300 cm^{-1}, essentially the same as our previously calculated value. This value also lies close to estimates from molecular beam experiments, which place the IVR threshold near 1200 cm^{-1}.[33] Interestingly, the IVR transition lies above our best estimate for the ZPE-corrected barrier given in Table 3. This implies that the present situation is quite unusual, though not unique,[14] in that the threshold behavior is actually controlled by IVR. This surprising fact could imply that the accuracy of the barrier we have used is not as important as one would usually expect. In particular, the measured energy threshold for isomerization may not reflect the actual barrier height. Again, we note that measured rates of photoisomerization in supersonic jets are very slow near and below 1300 cm^{-1}, 0.1 ns^{-1} or lower, consistent with either restricted or very slow IVR. The values we computed for the IVR thresholds in the relevant isotopomers may be found in Table 2.

For energies above the transition (apart from a very narrow region of energy just above it[51]) LRMT uses perturbation theory to estimate the IVR rate. The rate of energy transfer from a state on the energy shell is then[51]

$$k_{IVR}(E) = \frac{2\pi}{\hbar}\sum_Q |V_Q|^2 \rho_Q(E) \tag{5}$$

where Q labels the order of coupling, and is calculated with eq 4c. The local density of states, $\rho_Q(E)$, can again be found by direct count, and the magnitude of anharmonic coupling is estimated using eq 4. Using the calculated IVR rate above 1300 cm^{-1}, we calculate the transmission coefficient using eq 2a. We find the rate of IVR to be of the order 1 ps^{-1} above about 2000 cm^{-1}, close to our previous results[16] and similar to IVR rates measured at this energy in supersonic jets.[35] The resulting IVR rates for the four isotopomers are shown in Figure 6. The IVR rates are not strongly affected by isotopic substitution.

Using the imaginary frequency at the transition state for the barrier crossing frequency and the IVR rates discussed above, we have computed the RRKM rate with and without dynamical corrections for d_0 stilbene. Because of the uncertainty in the barrier height as discussed above, we compute the rates with

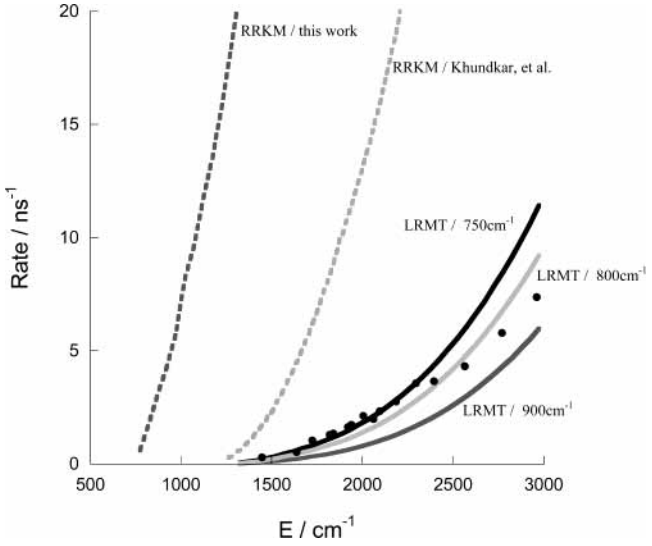

Figure 7. Comparison of the RRKM (dotted line) and LRMT (solid line) rates for trans → cis isomerization on S_1 in d_0-stilbene. Parameters in the rate theories are obtained from the ab initio calculations detailed in the text. Previous RRKM results of ref 18 are shown as the gray dashed line. Our RRKM rates are much larger than previous RRKM rates because of the low barrier height we compute. Experimental results from ref 10 are plotted as solid circles. LRMT rates are plotted for several barrier heights − 750 cm^{-1} (black solid line), 800 cm^{-1} (light gray solid line), and 900 cm^{-1} (dark gray solid line).

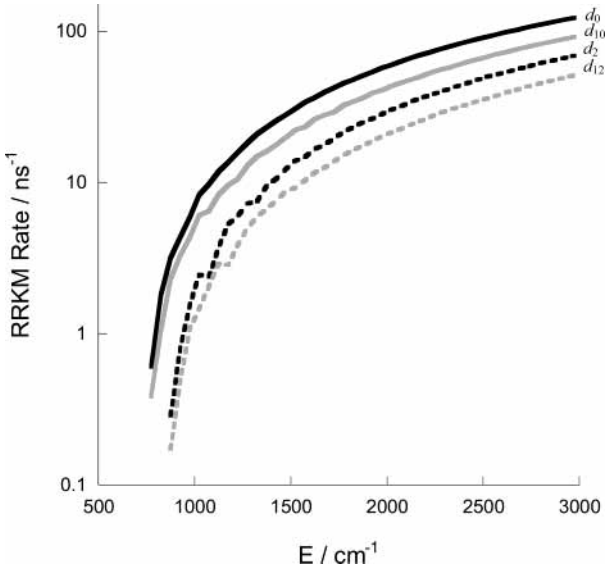

Figure 8. RRKM isomerization rates computed for four isotopomers of *trans*-stilbene. The order obtained is largely determined by the zero-point energy corrections to the barrier height.

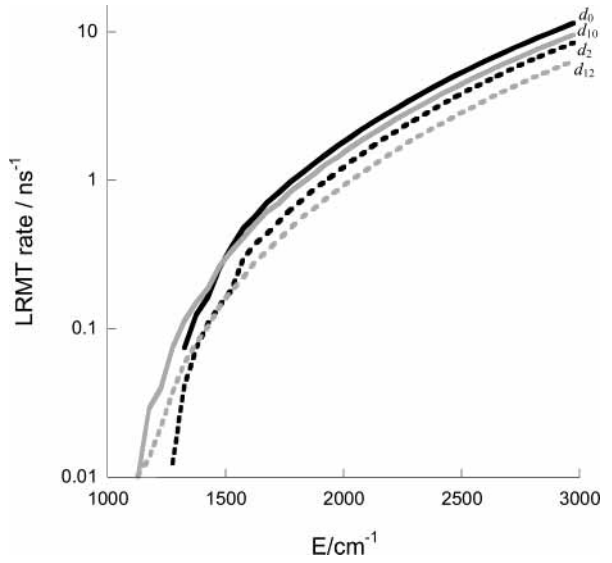

Figure 9. LRMT rates for isomerization on S_1 for four isotopomers of *trans*-stilbene. The order is exactly as determined experimentally.

LRMT dynamical corrections for three different choices of the zero-point-corrected barrier height − our best estimate of 750 cm^{-1} and two slightly larger values (800 and 900 cm^{-1}), corresponding to bare barriers of 1347, 1397, and 1497 cm^{-1}, respectively. The results are plotted in Figure 7 together with experimental results for stilbene isomerization in supersonic jets by Felker and Zewail,[10] and the results of a previous RRKM study.[18] The RRKM rate we compute is in much worse agreement with experiment than previous workers have found using RRKM theory. This is because the threshold is very low, as a consequence of the low barrier found in our calculations. However, after accounting for the finite rate of IVR, very good agreement of theory with experiment is obtained. All three of the barrier heights chosen lead to agreement within a factor of 2 over the depicted energy range. The best agreement is obtained with a barrier height of 800 cm^{-1}, which is very close to our computed barrier height and well within the expected error for the barrier height from our electronic structure treatment. However, we avoid any ad hoc adjustment of the barrier in the following and use the best ab initio barrier (1347 cm^{-1} before ZPE corrections, which are taken from Table 2 for the appropriate isotopomer) in all the rate calculations unless explicitly specified. For the energy range shown, quantum energy flow and not the barrier crossing frequency determines the rate at which reactants form products from transition states.

Figure 8 compares the RRKM rates for different isotopomers using the ab initio data. The ordering of the rates is exactly as found experimentally, and this can be traced back to the zero-point energy effects on the barrier height. The fact that an RRKM treatment already gets this right implies that it is *not* the isotope dependence of IVR which governs the unusual ordering of rates for these isotopomers. Indeed the ordering of IVR rates seen in Figure 6 could hardly reorder the RRKM rates which would be obtained ignoring the isotope dependence of the ZPE corrections. Thus, one should immediately ask whether the RRKM ordering of isotopomer rates is preserved when IVR is accounted for. Indeed, it is. This is shown in Figure 9. Although the ordering obtained with an RRKM method is preserved, the absolute value of the rates decreases tremendously, and the threshold for reaction is changed. Finally, we plot the experimental and predicted rates for all four isotopomers in Figure 10. The d_0/d_2 and d_{10}/d_{12} are shown in separate panels for clarity. Although the rates are in error by up to a factor of 2 at certain energies, we remind the reader that this comparison contains *no* adjustable parameters—all input comes from the ab initio calculations or the scaling rules of Gruebele. We find the agreement achieved to be astonishing. However, we should not be content until the pressure dependence can also be explained in the current framework. We turn to this point next.

4. Thermal Isomerization Rate

The rate of vibrational energy flow in stilbene will be influenced by the rate of collisions. Using a strong collision model, the microcanonical rate is given by $k(E) = \kappa(E)k_{RRKM}(E)$, where the transmission coefficient that incorporates collisions is

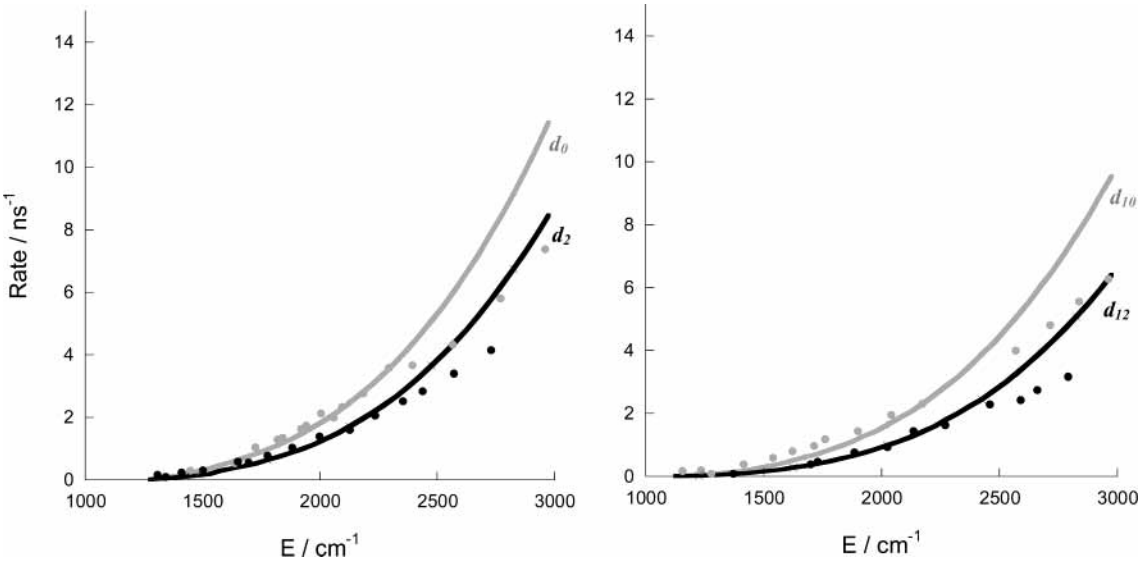

Figure 10. Direct comparison of LRMT and experimental isomerization rates for *trans*-stilbene isotopomers. Left panel compares d_0 (dark gray, circles) and d_2 (black, diamonds) rates. Right panel compares d_{10} (dark gray, circles) and d_{12} (black, diamonds) rates. LRMT rates are depicted as solid lines and experimental points are depicted as symbols. This comparison involves *no* adjustable parameters.

$$\kappa(E) = \frac{k_{\mathrm{IVR}}(E) + \alpha}{k_{\mathrm{IVR}}(E) + \alpha + \nu_{\mathrm{R}}(E)} \tag{6}$$

and α is the collision frequency. This again assumes exponential IVR. Then the thermal rate of isomerization is

$$k(T) = Q^{-1} \int_{E_0}^{\infty} \frac{\mathrm{d}E\ \alpha k(E) \rho(E) e^{-\beta E}}{\alpha + k(E)} \tag{7}$$

where $Q = \int \rho(E)\ \exp(-\beta E)\ \mathrm{d}E$. The relation between pressure and collision frequency has been estimated to be $\alpha = 0.025$ ps^{-1}/atm,[11] based on the sizes of stilbene and methane molecules. However, collision frequencies based on hard sphere approximations neglect electrostatic effects such as polarizability. The work of Meyer, Schroeder, and Troe[33] suggests that this may be important in the present case, since the stilbene isomerization rate differs significantly in Ar and CH_4 buffer gases which have very nearly equal hard sphere diameters but quite different polarizabilities. Thus, we use a collision frequency of $\alpha = 0.2$ ps^{-1}/atm, which amounts to an increase of the collision diameter from the hard sphere value by a factor of 2.8. With this collision frequency, our calculations of the thermal isomerization rate match the measured rates remarkably well. This collision frequency is the same as used in previous work,[16] and we have made no attempt to treat it as a fitting parameter. However, there is no firm justification for the particular value chosen and one might achieve better agreement by modifying it. This remains an open point for future investigation, but it is probably more productive to compute the collision frequency directly from a dynamics simulation which incorporates polarization effects.

We have calculated $k(T)$ at collision frequencies corresponding to a range from about 1 to 100 atm. The results (black line) are plotted in Figure 11, together with the Balk−Fleming data. Balk and Fleming[11,12] found the isomerization rate to vary by about a factor of 13 over this range. We find a factor of 7 and reasonable quantitative agreement with Balk and Fleming. We also plot the results (gray line) obtained using a barrier height of 800 cm^{-1} after ZPE corrections. The variation of the isomerization rate is barely affected and one concludes that the agreement obtained is not overly sensitive to the barrier height.

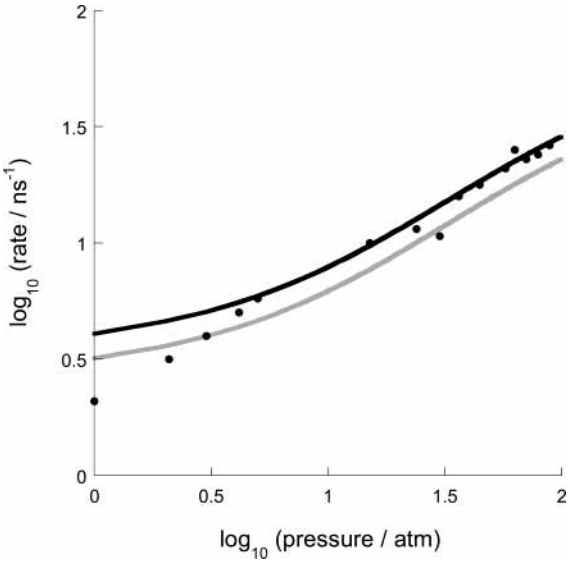

Figure 11. Experimental (filled circle) and LRMT (solid black line) thermal rates for d_0-stilbene isomerization. LRMT results with a slightly modified barrier height (800 cm^{-1} after ZPE corrections) are shown for comparison (gray solid line).

We might still consider other factors that could influence the isomerization rate in addition to the dynamical corrections to the RRKM rate due to sluggish quantum energy flow. One possibility, argued by Troe and co-workers for some time,[20,29] is that the reaction barrier might be influenced by the solvent, particularly at higher pressures, above about 10 atm, where clustering could occur. At low pressures, Gershinsky and Pollak[19] have suggested that the thermal rate might be influenced by possible cooling of the reactant upon photoexcitation from S_0 to S_1. Indeed, spectroscopic evidence for cooling at pressures around 1 atm has been recently reported.[36]

Following Gershinsky and Pollak,[19] we can approximately estimate the possible effects of cooling on the isomerization rate by calculating the excess vibrational energy of the molecule

$$\langle E_v \rangle = \sum_i \frac{\hbar\omega_i}{e^{\beta\hbar\omega_i} - 1} \tag{8}$$

Since the vibrational modes of S_1 are generally slightly lower than the S_0 modes (see Table 1), the temperature upon photoexcitation to S_1 must be effectively lower so that the excess energy in S_1 matches that of S_0. Using the S_0 and S_1 frequencies in Table 1, we find a cooling of about 3 K. This is too small to change the rate significantly. Gershinsky and Pollak's theory suggests there may be a larger cooling than this estimate that is based on the adiabatic expansion of the phase space, owing to specific dynamical quantum effects depending on the width of the laser pulse, etc.[19,56] In our view, such specific dynamics would require nonergodicity or at least slow IVR. Thus we may entertain the possibility of such greater cooling. For example, cooling of 10 K would lower the isomerization rate (including IVR corrections) at 1 atm by about 20%, so that overall the isomerization rate would increase by perhaps a factor of 10. This would come quite close to the observed increase in the rate of photoisomerization with pressure from 1 to 100 atm. A detailed calculation of the cooling effects accounting for slow but nonzero IVR would thus be most welcome and should be accessible using LRMT.

5. Concluding Remarks

We have used multireference ab initio methods to compute a new potential energy surface for S_1 *trans*-stilbene. Using the new set of normal-mode frequencies computed for the reactant and transition state on this surface, we have calculated the rate of photoisomerization of *trans*-stilbene. We find, consistent with most of the earlier work, that dynamical corrections to RRKM theory are critical for accurately predicting microcanonical and thermal rates of photoisomerization, much as seems to be the case for other conformational changes with low barriers for several other modest-sized molecules.[2−8] RRKM calculations yield microcanonical rates that are much larger than measured rates in supersonic jets. This overestimate is accounted for using a dynamical correction to microcanonical transition state theory, which itself can be calculated by local random matrix theory (LRMT) without adjusting the potential energy surface. The dynamical correction arises because quantum mechanical energy flow in to and out of the transition states of stilbene is slower than the vibrational frequency for the transition from activated complex to product. Using LRMT and the new vibrational frequencies, we have calculated the rate of IVR to be on the order of 1 ps^{-1}, consistent with measured rates of IVR in stilbene.[10,57] The discrepancy between IVR rates and the frequency of the reaction mode should be very common for reactions of large molecules over low barriers.[2−8] Thus we are convinced that dynamical corrections to RRKM theory are required to predict measured rates of isomerization of a variety of moderate-sized organic molecules,[2−8] with the photoisomerization of *trans*-stilbene apparently being no exception. Quantum mechanical energy flow plays a significant role in establishing the microcanonical reaction rate because at energies not very far above a low-energy barrier most vibrational modes of a modest-sized molecule are excited to only very low levels if at all. Anharmonic coupling of such low-energy states is relatively small, and the energy flow rate, if there is energy flow at all, is generally quite slow compared to vibrational motions of the reactant.

Our best estimate for the barrier height is significantly lower than previous accepted values. At the same time, we find the threshold energy for IVR to be significantly larger than the barrier height, implying that the measured energy threshold is not a good measure of the barrier height. Even so, the barrier height used will strongly affect isomerization rates once the energy is larger than the threshold. Despite the expected difficulties in computing an excited-state barrier to the level of accuracy required in a rate calculation, we find that using LRMT with no adjustable parameters leads to very good agreement with experimental isomerization rates (Figures 7, 10, and 11). As shown in Figure 7, this agreement is improved somewhat with a slight adjustment (50 cm^{-1}) of the barrier height, well within the expected uncertainties in the ab initio methods.

Some of the results presented here depend on the choice for the frequency of the reaction coordinate, ν_R. At energies not very far above the barrier, microcanonical rates are not very sensitive to this choice since in this range of energies the reaction rate is controlled by IVR. However, the thermally averaged rate does depend on this choice, particularly at higher pressures, since a larger RRKM limit is reached for larger ν_R. Experiment has provided a lower limit of $\nu_R \approx 160$ cm^{-1},[31] and values of 200−400 cm^{-1} have generally been assigned for this mode.[25] We find an imaginary frequency of ≈600 cm^{-1} from the ab initio calculations and have used this value in our rate calculations. We find the same qualitative trends in the pressure dependence of the reaction rate as observed by Balk and Fleming.[11,12] We obtain an overall rise in the thermal reaction rate from 1 to 100 atm by a factor of 7, reasonably close to the observed factor of 13.

The intriguing suggestion that laser cooling contributes to the rise in the reaction rate with pressure remains a possibility. We found that the effect of cooling at low pressures probably should be small, possibly lowering the rate by a few percent. A complete theory of cooling incorporating restricted or slow energy flow, however, may give a bigger effect.[58]

Likewise, the possibility of effects arising from van der Waals clustering with the buffer gas cannot be ruled out entirely. Felicitously, this possibility can be probed also by detailed quantum chemical calculations on stilbene in such clusters. Our intuition, however, does not lead us to expect as large variations in the barrier as Troe and co-workers invoke.[20,29]

In conclusion, the best available potential energy surface when treated using a theory accounting for dynamic corrections to RRKM explains the observations on *trans*-stilbene photoisomerization with good accuracy without using adjustable constants. Ockham's Razor presently then forces us to eliminate as dominating features the many speculative suggestions that are needed to explain the data using RRKM theory alone. We conclude that *trans*-stilbene photoisomerization may well ultimately join the textbooks as an example of a non-RRKM process.

Acknowledgment. We thank Prof. Martin Gruebele for helpful discussions and comments on the manuscript. Spirited discussions over the cooling effect with Eli Pollak are gratefully acknowledged. D.M.L. acknowledges support from the National Science Foundation (NSF CHE-0112631), the Camille and Henry Dreyfus Foundation and Research Corporation. T.J.M. acknowledges support from the National Science Foundation (NSF CHE-02-311876), the David and Lucille Packard Foundation and the Camille and Henry Dreyfus Foundation. P.G.W.'s work on quantum energy flow has been supported by the National Science Foundation. P.G.W. would like to dedicate this paper to Charles Parmenter, who has contributed greatly to our understanding of the quantum mechanics of energy redistribution in molecules. He also likes to take this opportunity to thank Prof. Parmenter for his advice to him as an undergraduate, especially about learning Russian. No theorist after the end of the Cold War can run his research group without a basic knowledge of that language.

Supporting Information Available: Text discussing calculations of and tables of the unscaled frequencies at S_0 minimum, S_1 minimum, and trans → cis isomerization transition state for d_0, d_2, d_{10}, and d_{12} isotopomers and Cartesian coordinates of the trans → cis isomerization transition state and excited state trans minimum. This material is available free of charge via the Internet at http://pubs.acs.org.

References and Notes

(1) Baer, T.; Hase, W. L. *Unimolecular Reaction Dynamics: Theory and Experiments*; Oxford University Press: New York, 1996.
(2) Dian, B. C.; Longarte, A.; Zwier, T. S. *Science* **2002**, *296*, 2369.
(3) Baer, T.; Potts, A. R. *J. Phys. Chem.* **2000**, *104A*, 9397.
(4) Hasha, D. L.; Eguchi, T.; Jonas, J. *J. Am. Chem. Soc.* **1982**, *104*, 2290.
(5) McWhorter, D. A.; Pate, B. H. *J. Phys. Chem.* **1998**, *102A*, 8786.
(6) McWhorter, D. A.; Pate, B. H. *J. Phys. Chem.* **1998**, *102A*, 8795.
(7) McWhorter, D. A.; Hudspeth, E.; Pate, B. H. *J. Chem. Phys.* **1999**, *110*, 2000.
(8) Keske, J. C.; Pate, B. H. *Annu. Rev. Phys. Chem.* **2000**, *51*, 323.
(9) Syage, J. A.; Lambert, W. R.; Felker, P. M.; Zewail, A. H.; Hochstrasser, R. M. *Chem. Phys. Lett.* **1982**, *88*, 266.
(10) Felker, P. M.; Zewail, A. H. *J. Phys. Chem.* **1985**, *89*, 5402.
(11) Balk, M. W.; Fleming, G. R. *J. Phys. Chem.* **1986**, *90*, 3975.
(12) Fleming, G. R.; Courtney, S. H.; Balk, M. W. *J. Stat. Phys.* **1996**, *42*, 83.
(13) Chandler, D.; Kuharski, R. A. *Faraday Discuss.* **1988**, *85*, 329.
(14) Leitner, D. M. *Int. J. Quantum Chem.* **1999**, *75*, 523.
(15) Nordholm, S. *Chem. Phys.* **1989**, *137*, 109.
(16) Leitner, D. M.; Wolynes, P. G. *Chem. Phys. Lett.* **1997**, *280*, 411.
(17) Nordholm, S.; Back, A. *Phys. Chem. Chem. Phys.* **2001**, *3*, 2289.
(18) Khundkar, L. R.; Marcus, R. A.; Zewail, A. H. *J. Phys. Chem.* **1983**, *87*, 2473.
(19) Gershinsky, G.; Pollak, E. *J. Chem. Phys.* **1997**, *107*, 812.
(20) Schroeder, J.; Steinel, T.; Troe, J. *J. Phys. Chem.* **2002**, *106A*, 5510.
(21) Warshel, A. *J. Chem. Phys.* **1975**, *62*, 214.
(22) Warshel, A.; Karplus, M. *J. Am. Chem. Soc.* **1972**, *94*, 5612.
(23) Negri, F.; Orlandi, G. *J. Phys. Chem.* **1991**, *95*, 748.
(24) Vachev, V. D.; Frederick, J. H.; Grishanin, B. A.; Zadkov, V. N.; Koroteev, N. I. *Chem. Phys. Lett.* **1993**, *215*, 306.
(25) Vachev, V. D.; Frederick, J. H.; Grishanin, B. A.; Zadkov, V. N.; Koroteev, N. I. *J. Phys. Chem.* **1995**, *99*, 5247.
(26) Gagliardi, L.; Orlandi, G.; Molina, V.; Malmqvist, P.-A.; Roos, B. O. *J. Phys. Chem.* **2002**, *106A*, 7355.
(27) Watanabe, H.; Okamoto, Y. A., S.; Furuya, K.; Sakamoto, A.; Tasumi, M. *J. Phys. Chem.* **2002**, *106A*, 3318.
(28) Foresman, J. B.; Head-Gordon, M.; Pople, J. A.; Frisch, M. J. *J. Phys. Chem.* **1992**, *96*, 135.
(29) Troe, J. *Chem. Phys. Lett.* **1985**, *114*, 241.
(30) Waldeck, D. H. *Chem. Rev.* **1991**, *91*, 415.
(31) Lee, M.; Holton, G. R.; Hochstrasser, R. M. *Chem. Phys. Lett.* **1985**, *118*, 359.
(32) Courtney, S. H.; Balk, M. W.; Phillips, L. A.; Webb, S. P.; Yang, D.; Levy, D. H.; Fleming, G. R. *J. Chem. Phys.* **1988**, *89*, 6697.
(33) Meyer, A.; Schroeder, J.; Troe, J. *J. Phys. Chem.* **1999**, *103A*, 10528.
(34) Beddard, G. S.; Fleming, G. R.; Gijzeman, O. L.; Porter, G. *Proc. R. Soc. London, Ser. A* **1974**, *340*, 519.
(35) Felker, P. M.; Lambert, W. R.; Zewail, A. H. *J. Chem. Phys.* **1985**, *82*, 3003.
(36) Warmuth, C.; Milota, F.; Kauffmann, H. F.; Wadi, H.; Pollak, E. *J. Chem. Phys.* **2000**, *112*, 3938.
(37) Docken, K. K.; Hinze, J. *J. Chem. Phys.* **1972**, *57*, 4928.
(38) Roos, B. O. The Complete Active Space Self-Consistent Field Method and its Applications in Electronic Structure Calculations. In *Advances in Chemical Physics: Ab Initio Methods in Quantum Chemistry II*; Lawley, K. P., Ed.; John Wiley and Sons Ltd.: London, 1987; p 399.
(39) Grabo, T.; Petersilka, M.; Gross, E. K. U. *J. Mol. Struct. (THEOCHEM)* **2000**, *501*, 353.
(40) Tozer, D. J.; Handy, N. C. *Phys. Chem. Chem. Phys.* **2000**, *2*, 2117.
(41) Celani, P.; Werner, H.-J. *J. Chem. Phys.* **2000**, *112*, 5546.
(42) Hehre, W. J.; Ditchfield, R.; Pople, J. A. *J. Chem. Phys.* **1972**, *56*, 2257.
(43) Werner, H.-J.; Knowles, P. J.; Amos, R. D.; Bernhardsson, A.; Berning, A.; Celani, P.; Cooper, D. L.; Deegan, M. J. O.; Dobbyn, A. J.; Eckert, F.; Hampel, C.; Hetzer, G.; Korona, T.; Lindh, R.; Lloyd, A. W.; McNicholas, S. J.; Manby, F. R.; Meyer, W.; Mura, M. E.; Nicklass, A.; Palmieri, P.; Pitzer, R.; Rauhut, G.; Schütz, M.; Stoll, H.; Stone, A. J.; Tarroni, R.; Thorsteinsson, T. MOLPRO 2000.1, 2000.
(44) Frisch, M. J.; Trucks, G. W.; Schlegel, H. B.; Scuseria, G. E.; Robb, M. A.; Cheesman, J. R.; Zakrzewski, V. G.; Montgomery, J. A., Jr.; Stratmann, R. E.; Burant, J. C.; Dapprich, S.; Millam, J. M.; Daniels, A. D.; Kudin, K. N.; Strain, M. C.; Farkas, O.; Tomasi, J.; Barone, B.; Cossi, M.; Cammi, R.; Mennucci, B.; Pomelli, C.; Adamo, C.; Clifford, S.; Ochterski, J.; Petersson, G. A.; Ayala, P. Y.; Cui, Q.; Morokuma, K.; Rega, N.; Salvador, P.; Dannenberg, J. J.; Malick, D. K.; Rabuck, A. D.; Raghavachari, K.; Foresman, J. B.; Cioslowski, J.; Oritiz, J. V.; Baboul, A. G.; Stefanov, B. B.; Liu, G.; Liashenko, A.; Piskorz, P.; Komaromi, I.; Gomperts, R.; Martin, R. L.; Fox, D. J.; Keith, T.; Al-Laham, M. A.; Peng, C. Y.; Nanayakkara, A.; Challacombe, M.; Gill, P. M. W.; Johnson, B.; Chen, W.; Wong, M. W.; Andres, J. L.; Gonzalez, C.; Head-Gordon, M.; Replogle, E. S.; Pople, J. A. *Gaussian 98*; revision A.11 ed.; Gaussian, Inc.: Pittsburgh, PA, 2002.
(45) Hehre, W. J.; Radom, L.; Schleyer, P. v. R.; Pople, J. *Ab Initio Molecular Orbital Theory*; John Wiley and Sons: New York, 1986.
(46) Quenneville, J.; Martínez, T. J. *J. Phys. Chem.* **2003**, *107A*, 829.
(47) Pople, J. A.; Head-Gordon, M.; Fox, D. J.; Raghavachari, K.; Curtiss, L. A. *J. Chem. Phys.* **1989**, *90*, 5622.
(48) Csaszar, A. G.; Allen, W. D.; Schaefer, H. F., III *J. Chem. Phys.* **1998**, *108*, 9751.
(49) Bigwood, R.; Gruebele, M.; Leitner, D. M.; Wolynes, P. G. *Proc. Natl. Acad. Sci.* **1998**, *95*, 5960.
(50) Bolton, K.; Nordholm, S. *Chem. Phys.* **1996**, *203*, 101.
(51) Leitner, D. M.; Wolynes, P. G. *J. Phys. Chem.* **1997**, *101A*, 541.
(52) Logan, D. E.; Wolynes, P. G. *J. Chem. Phys.* **1990**, *93*, 4994.
(53) Bigwood, R.; Gruebele, M. *Chem. Phys. Lett.* **1995**, *235*, 604.
(54) Pearman, R.; Gruebele, M. *J. Chem. Phys.* **1998**, *108*, 6561.
(55) Madsen, D.; Pearman, R.; Gruebele, M. *J. Chem. Phys.* **1997**, *106*, 5874.
(56) He, Y.; Pollak, E. *J. Chem. Phys.* **2002**, *116*, 6088.
(57) Schultz, S.; Qian, J.; Jean, J. M. *J. Phys. Chem.* **1996**, *101A*, 1000.
(58) After reading an earlier version of this paper, Pollak has communicated to us preliminary calculations using the surfaces reported in this paper that leave open the possibility of cooling greater than our 3 K estimate.